arXiv:cond-mat/0106280v1 [cond-mat.mtrl-sci] 14 Jun 2001

Morphology–transitions at vicinal Cu–surfaces based on entropic step–step interaction and diffusion along steps

Heike Emmerich
Max-Planck-Institut für Physik komplexer Systeme, Nöthnitzer Str. 38, D 01187 Dresden, Germany

An extension of the Burton–Cabrera–Frank model [Phil. Trans. R. Soc. London, Ser. A **243**, 299 (1951)] including diffusion along steps and entropic step–step interaction is introduced. This extended model is successfully applied to simulate experiments done in the group of H.–J. Ernst at CEA Saclay, France, for vicinal Cu surfaces. In particular, the rise of two qualitatively different morphologies can be explained by the competition of growth directions implied by the four distinct driving and restoring forces of the model. Each of those forces sets a length scale for the dominant mode of a developing step instability. This explains that the wavelengthes of meandering–instabilities observed at vicinal surfaces experimentally are usually larger than the one predicted by Bales and Zangwill [Phys. Rev. B **41**, 5500 (1990)] theoretically.

During molecular beam epitaxy (MBE) appropriate conditions for the controlled growth of vicinal surfaces can be fine–tuned. This way one tries to fabricate either atomistically flat or nanostructured surfaces. The ability to exert control on structuring along the growth direction and fabricate substrates with smallest–scale–built–in periodicies normal to the surface is well advanced. Efforts to still enhance abilities to determine functional properties of a grown substrate now focus on the lateral structuring within one layer of growth. One direction along this line is to make use of the inherent instabilities due to the dynamics of the growth process itself [1]. A necessary first step is to understand the basic wavelengthes of those inherent instabilities just as well as the kind of morphologies which will develop.

More then ten years ago, Bales and Zangwill [2] predicted that a growing vicinal surface should undergo a step meandering instability when kinetic step edge barriers suppress the attachments of atoms to decending steps [3]. According to their analysis, a straight step is linearly unstable against perturbations with wavelengths larger then $\lambda_c = 2\pi(2\Gamma L_\Delta)$ and a fastest growing wavelength at $\lambda_u = \sqrt{2}\lambda_c$ ($\Gamma = \frac{\Omega\gamma}{k_B T}$, $L_\Delta = \frac{Dc_{eq}}{Fl^2}$). Here F denotes the deposition rate, D the diffusion constant for diffusion *on* the terraces and c_{eq} the equilibrium concentration, γ the step stiffness, Ω the atomic area and $k_B T$ the termal energy. Even though the meandering instability has meanwhile been observed in experiments and simulations [4], the quantitative prediction of the Bales–Zangwill analysis could not be recovered in many of those experimental findings. This point received much interest in view of the recent experiments by Maroutian *et al.* [5] at CEA Saclay. Analytical efforts to resolve the disagreement between experimental measurements and theoretical prediction led to a precise study of the limit of desorptionless growth. For to derive a single evolution equation in the weakly nonlinear regime this case has the interesting feature of displaying a singularity in the spirit of multiscale expansion [6]. As a result, meander–wavelengthes larger than the ones predicted by Bales and Zangwill can be explained, however, without reaching the order of experimental observations. Other efforts center around the investigation of an extra diffusion current *along* step edges [7]. Such a current triggers an asymmetry in energy barriers for atoms attaching at kinks from different step edge directions, the so called Kink Ehrlich–Schwoebel effect (KESE) [8]. KESE can either destabilize or stabilize steps depending on whether the slope of the meander–instability is greater or less than one. In [5] calculations including a stabilizing KESE–current along steps were compared to the further thesis that islands might nucleate at step edges and thereby constitute a still different wavelength of instability. It appeared that the latter thesis fits best to the experimental wavelength–values.

New light was shed on these investigations by experiments which revealed that a morphology qualitatively different from the meandering one can develop on vicinal surface as well, with growth conditions being exactly the same as for the meandering–morphology except a different angle of miscut [9]. It can be characterized by the absence of one global growth direction and thereby resembles the so called *degenerated morphology* [10]. Thus the insufficiency of theoretical approaches to explain the difference between the wavelength of instability predicted by Bales and Zangwill and the one observed experimtentally was extended by their failure to explain this *degenerated morphology*. Note that the surface of the in–phase–meandering morphology displayed in the STM topograph in Fig. 1(b) [5] was wrongly identified as Cu(1,1,17) and is in fact a Cu(0,2,24) surface [11]. The true Cu(1,1,17) on the other hand is the one to display a *degenerated morphology* [9].

In this letter I will introduce a novel model which can explain the rise of two different morphologies as well as their basic wavelengthes including KESE currents plus entropic step–step repulsion in the classical Burton–Cabrera–Frank (BCF) model [12]. It is the competition between the destabilizing and the stabilizing forces combined in this extended BCF model (EBCF model) which

results into two different kinds of morphologies depending on the difference in magnitude of orthogonal driving forces. A careful analysis of this interaction also reveals a new basic wavelength of instability which is in the order of the experimental observations.

To get an impression of the basic ideas underlaying the EBCF let us start with the one sided BCF model, i.e. the model formulated by Burton, Cabrera and Frank in 1951 for the case of complete supression of attachment of adatoms to decending steps. This one–sided BCF model constitutes a *moving boundary problem* of a diffusion–relaxation equation for the dynamics of the adatoms on the terraces and two boundary conditions for the conservation of mass and the conservation of energy at the steps, respectively:

$$\partial_t c = D\nabla^2 c - \frac{1}{\tau}c + F \tag{1}$$

$$c_{eq} = c^0_{eq} \cdot (1 + \kappa\Omega\gamma/k_B T) \tag{2}$$

$$v_n = D\Omega\frac{\partial c}{\partial n}. \tag{3}$$

Here c denotes the areal adatom density, c^0_{eq} the equilibrium concentration for a straight step and κ the step curvature. Equations (2) and (3) are to be evaluated at the front of each step. For vicinal Cu surfaces in the temperature range of the experiments under discussion a current involving the diffusion coefficient D_m along the kinked steps is operative [7]. Following the notation of Pierre–Louis *et al.* [8] this diffusion along steps plus its anisotropy due to KESE can be included in the *moving boundary problem* above extending Eq.(3) by $-\partial_x J$, with $J = J_k + J_e$ (J_k, J_e as in Eq.(2)–(4) in the paper of Pierre–Louis *et al.*). Note that unlike the authors of [8] I consider γ to be the step stiffness instead of the line tension as the precise measure of the step's tendency to straighten and thus reduce its kink density. As a consequence it is taken into account that just as surface undergoing a faceting instability develops into the surface–tension–minimizing morphology, instabilities at step edges have ideal orientations which can minimize line tension as well. This is crucial for the model since this is exactly the point in which the Cu(1,1,17) and the Cu(0,2,24) vicinal surface differ. Both surfaces are made up of (001) terraces of monoatomic hight and mean terrace width $l = 21.7$Å. However, for the Cu(1,1,17) surface straight step edges before the growth of instabilities are parallel to the <100> direction, whereas they are parallel to <110> in the case of Cu(0,2,24). As a consequence the direction of minimal step stiffness, which can be determined to be in <130> via an embedded atom method (in analogy to [13] for surfaces), encloses an angle of appr. 63.5^0 with the straight steps in case of Cu(0,2,24), whereas the angle is appr. 71.5^0 in the case of Cu(1,1,17). Since growth proceeds in the direction of minimal step stiffness, these are the orientations for the initial formation of the instabilities. They trigger destabilizing J_k currents of different magnitudes along the step edge forming in this direction. For to evaluate J_k a quantitative value for the KESE–length L_s (ref. [8], Eq.(3)) is required. The relevant kink energy barrier is the one directed in $<\bar{1}10>$, giving 0.518eV using an effective medium theory potential [14,20]. The diffusion barrier for the jump of a single adatom along the step edge in this direction is 0.399eV [14,20], leading to a KESE–length L_s of 201.2. The resulting j_k current densities for Cu(0,2,24) versus Cu(1,1,17) differ by one order of magnitude: for Cu(0,2,24) j_k takes a value of $7.118 \cdot 10^{-7}(\text{Å}^2\text{s})^{-1}$, whereas at Cu(1,1,17) $j_k = 6.396 \cdot 10^{-8}(\text{Å}^2\text{s})^{-1}$. Despite their different magnitudes in both cases KESE currents are destabilizing, favoring unsaturating amplitude growth. Wavelengthes of instabilities turn out to be even less then in the BCF model. As a consequence taking into account KESE as only additional driving force in the BCF model is not well suited to explain the experimental work by T. Maroutian and coauthors. An obvious antagonist of the destabilizing KESE is the repulsion due to the succeeding step. Entropic just as well as elastic interactions [16] have to be taken into account. Since the step interaction engergy A considering an elastic or a dipole momentum is small compared to the entropic repulsion in the temperature ranges under discussion [15], it is sufficient to extend Eq.(2) by taking into account the surpression of step wandering:

$$c_{eq} = c^0_{eq} \cdot (1 + \frac{\kappa}{k_B T} \cdot (\Omega\gamma + \frac{(\pi k_B T)^2}{6l^2\gamma})) \tag{$\tilde{2}$}$$

$$v_n = D\Omega\frac{\partial c}{\partial n} - \partial_x J \tag{$\tilde{3}$}$$

The additional term $(\pi k_B T)^2/6l^2\gamma$ is the step interaction parameter with l equal the width of the terraces. Equations (1), ($\tilde{2}$) and ($\tilde{3}$) constitute the extended BCF model (EBCF). Its simulation with T=280K, F=$3\cdot10^{-3}$ ML/s, l=21.7 Å, $D_m = 10^{-6}\text{cm}^2/\text{s}$, $c_{eq} = 8.208 \cdot 10^{-6}\text{Å}^{-1}$ and γ= 1.034·eV/Å yields the following two morphologies for the Cu(0,2,24) surface (Fig. 1) and the Cu(1,1,17) (Fig. 2), respectively.

The four components regulating growth of instabilities in the EBCF are

1. driving of growth via the gradient of the adatom diffusion field normal to the interface setting the length scale L_Δ for a primary wavelength of instability

2. restore via step stiffness (corresponding length scale: Γ)

3. driving of amplitude growth via KESE (length scale: L_s, ref. [8])

4. restore via entropic repulsion (length scale: $L_S = \frac{6\gamma l^2}{k_B T \pi^2}$) .

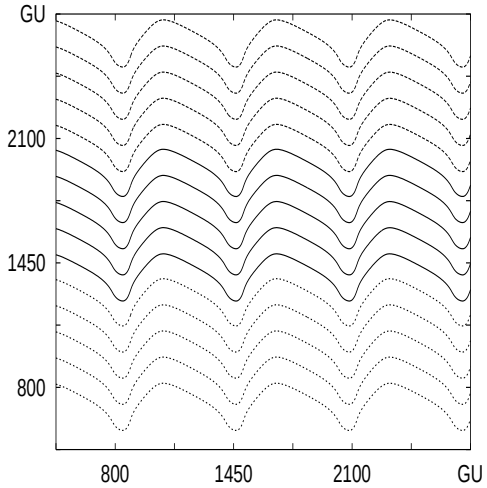

FIG. 1. In–phase meandering according to numerical simulations of EBCF. The parameters of the simulation are calibrated to Fig. 1(b) in [5]. GU referes to grid units of the underlaying numerical grid. A train of 15 steps with periodic boundary conditions in lateral direction is displayed. Horizontal boundary conditions are periodic as well. Space calibration leads to roughly 10 grid units corresponding to 1Å.

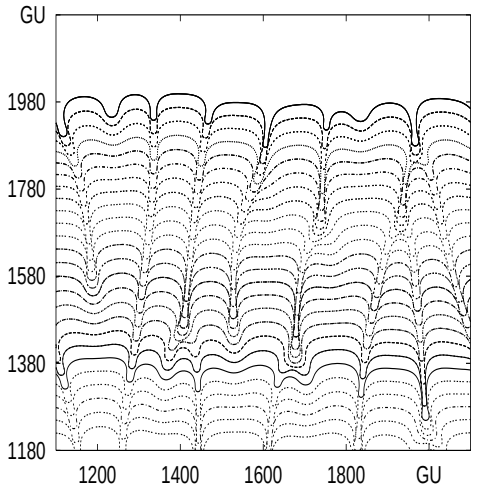

FIG. 2. The *degenerated* morphology as obtained in simulations. Same as in Fig.1 except a different scale of 1GU corresponding 1Å and taking into account the different vicinal (namely Cu(1,1,17) versus Cu(0,2,24)) via a different direction of minimal step stiffness and resulting different magnitude of KESE (refer to text). A train of 25 steps with first step growing towards infinity is displayed. Steps feel the infuence of overlapping fields [19]. This simulation result is in good agreement with the *degenerated* morphology recorded for Cu(1,1,17) after deposition of about 20 ML at F=$5{\cdot}10^{-3}$ ML/s at surface temperature 285 K via STM topography [9].

In the situation depicted by Fig. 2 the magnitude of the KESE current derivative $\partial_x J$ is neglectable small. The remaining forces due entropic and step stiffness effects act in directions perpendicular to each other. The result of this competition of prependicular forces of equal strength is the *degenerated morphology* as observed in other contextes with an analogous competition of driving forces [10].

In contrary in Fig. 1 the KESE current does contribute to the evolution of surface morphology. The magnitude of the driving force due to this current is of an order 10 smaller then the magnitude of the adatom diffusion field gradient in direction of minimal step stiffness. The precise factor is evaluated via simulation and reads 11.129 for the simulation run done for Fig. 1 averaged over 500 timesteps. Due to the dominance of L_Δ growth can proceed in the direction of minimal step stiffness.

For to understand the basic wavelength of the instability the two new length scales L_S and L_s, set by entropic interaction as in Eq.$(\tilde{2})$ and by an anisotrop diffusion current along the step as in Eq.$(\tilde{3})$ respectively, have to be taken into account. Eq.(1),$(\tilde{2})$ and $(\tilde{3})$ constitutes a system with a type I bifurcation [17]. It's dispersion relation can be evaluated in analogy to a dilute binary alloy undergoing directional solidification [18]. For $\Gamma \ll Ł_S$ the resulting expression in leading order reads

$$\lambda_u = \sqrt{2}\pi(\frac{L_\Delta \cdot \Gamma \cdot Ł_S}{4})^{1/3} + 2\sqrt{2}\pi\frac{\Gamma L_s}{3l_T}. \qquad (4)$$

It replaces Eq.(1) in [5]. Expr.(4) is sufficient in the most interesting temperature range 2.8 to 3.8 x $10^{-3}K^{-1}$. It displays deviations from an Arrhenius–type behaviour, which increase with increasing temperature. Nevertheless it is in good agreement with the experimental data (Fig. 3). Simulations of the EBCF model support this expression as well.

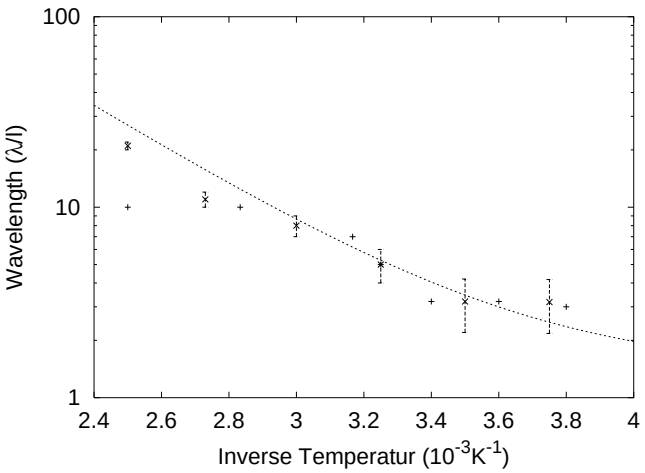

FIG. 3. The '+'–data points are taken from [5] and give the wavelength measurements recorded there. The full line is the solution of (4). Crosses with errorbars are data points obtained from simulation with the EBCF. There are limitations to a precise wavelength–measure in the simulations. Due to the horizontal periodic boundary conditions wavelengthes are always a divider of the system's width. Enlargening this system width systematically until the rise of a further cell as well as restricting the width until the extinction of one of the cells allows to find upper and lower bounds. Data points are the mean of these bounds which themselves are taken into account via the error bars. Thus each data point is a result of up to 15 simulations with different system widthes.

The extended BCF explains two relevant new results for growth at vicinal surfaces, namely the experimentally observed deviation from the Bales–Zangwill instability and the rise of a *degenerated morphology*. These results are related to experimental findings in the group of H.–J. Ernst. The new basic wavelength predicted theoretically from the EBCF–model can be observed as initial perturbation of the step at Cu(0,2,24) just as well as Cu(1,1,17) surfaces. The qualitative difference between their morphologies, i.e. whether a surface displays an in–phase–meandering (Cu(0,2,24)) or a *degenerated* structure (Cu(1,1,17)) after deposition of a few monolayers, depends on the magnitude of the angle between the direction of destabilizing and restoring force. Time scales for the development from initial perturbation to the full *degenerated* morphology could not be compared with experiments due to the lack of experimental data. It seems an interesting question whether *in situ* transitions from one morphology to the other can be obtained via a change in the ratio of driving forces (e.g. by lowering temperature during the experiment). If this morphology transition displays features which resemble a true phase transition remains to be investigated.

The diffusion–relaxation Eq.(1) is solved on a quadratic grid. The interface is discretized separatly by curvilinear segments and respective interpolations from the interface to the grid. Details of the scheme and its parallelization will be given in a further paper.

I thank T. Maroutian and M. Rusanen for sending me a STM–picture of the true Cu (1,1,17) surface–morpology as well as a respective preprint prior to publication. Comments by H. Müller–Krumbhaar to focus my attention on a precise understanding of the basic wavelength of instability arising in the EBCF–model are gratefully acknowledged. Part of the computations were done on the T3E and the Origin 3800 of the URZ at Dresden Technical University.

Note–The two surfaces (Cu(1,1,17) and Cu(0,2,24)) have also been modeled in [20] on the basis of a kinetic Monte Carlo algorithm without taking into account entropic repulsion. The agreement with experimental findings remains restricted, nevertheless it is a very precise study of the different effects of KESE at the different surfaces.

[1] J.–K. Zuo and J.F. Wendelken, Phys. Rev. Lett. **78**, 2791 (1997); H.–J. Ernst *et al., ibid.* **72**, 112 (1994); L.C. Jorritsma *et al., ibid.* **78**, 911 (1997); J.A. Stroscio *et al., ibid.* **75**, 4246 (1997); J.E. Van Nostrand *et al., ibid.* **74**, 1127 (1995)

[2] G.S. Bales, A. Zangwill, Phys. Rev. B **41**, 5500 (1990)

[3] R.L. Schwoebel, E.J. Shipsey, J. Appl. Phys. **37**, 3682 (1966)

[4] L. Schwenger, R.L. Folkerts, H.–J. Ernst, Phys. Rev. B **55**, R7406 (1997); J.E. Van Nostrand, S.J. Chey, D.G. Cahill, *ibid.* **57**, 12536 (1998); P. Tejedor, P. Šmilauer, B.A. Joyce, Microelectronics Journal **30**, 477 (1999); M. Rost, P. Šmilauer, J. Krug, Surf. Sci. **369**, 393 (1996); H. Emmerich *et al.*, J. Phys.: Condens. Matter **11**, 9985 (1999)

[5] T. Maroutian, L. Douillard, H.–J. Ernst, Phys. Rev. Lett. **83**, 4353 (1999)

[6] O. Pierre–Louis *et al.*, Phys. Rev. Lett. **80**, 4221 (1998); F. Gillet, O. Pierre-Louis, C. Misbah, Eur. Phys. J. B **18**, 519 (2000); J. Kallunki, J. Krug, Phys. Rev. E **62**, 6229 (2000)

[7] M. Giesen–Seibert *et al.*, Phys. Rev. Lett. **71**, 3521 (1993); **73**, E911 (1994); Surf. Sci. **329**, 47 (1995); K. Mussawisade, T. Wichmann, K.W. Kehr, Surf. Sci. **412/413**, 55 (1998)

[8] I.L. Aleiner, R.A. Suris, Sov. Phys. Solid State **34**, 809 (1992); Z. Zhang, M.G. Lagally, Science **276**, 377 (1997); J.G. Amar, Bull. Am. Phys. Soc. **43**, 851 (1998); O. Pierre–Louis, M.R. D'Orssogna, T.L. Einstein, Phys. Rev. Lett. **82**, 3661 (1999)

[9] T. Maroutian *et al.*; (to be published)

[10] F. Heslot, A. Libchaber, Phys. Scri. **T9**, 126 (1985); S. Akamatsu, G. Faivre, T. Ihle, Phys. Rev. E **51**, 4751 (1995)

[11] T. Maroutian *et al.*, *Erratum*; (to be published)

[12] W.K. Burton, N. Cabrera, F.C. Frank, Phil. Trans. R. Soc. London, Ser. A **243**, 299 (1951)

[13] D. Wolf, Surf. Sci. **226**, 389 (1990)

[14] J. Merikoski *et al.*, Surf. Sci. **387**, 167 (1997); J. Merikoski, T. Ala–Nissila, Phys. Rev. B **52**, R8715 (1995);

[15] H.–C. Jeong, E.D. Williams, Surf. Sci. **171**, 47 (1999) *and references within*

[16] B. Houchmandzadeh, C. Misbah, J. Phys. I France **5**, 685 (1995); C. Duport, P. Politi, J. Villain, J. Phys. I France **5**, 1371 (1995)

[17] M.C. Cross, P.C. Hohenberg, Rev. Mod. Phys., **65**, 851 (1993)

[18] W.W. Mullins, R.F. Sekerka, J. Appl. Phys. **35**, 444 (1964)

[19] F. Liu, H. Metui, Phys. Rev. E **49**, 2601 (1994)

[20] M. Rusanen, I.T. Koponen, J. Heinonen, T. Ala–Nissila, preprint, (2001)